Light-activated self-generation and parametric amplification for MEMS oscillators

M. Zalalutdinov, A. T. Zehnder, A. Olkhovets, S. Turner, L. Sekaric, B. Ilic, D. Czaplewski, J. M. Parpia, H. G. Craighead

Cornell Center for Material Research, Cornell University, Ithaca NY 14853

ABSTRACT

High-frequency microoptoelectromechanical systems (MOEMS) are proposed as active devices for radio frequency signal processing. Parametric amplification (PA), generation, frequency modulation and frequency conversion on the micromechanical level were demonstrated at MHz range by microfabricated single-crystal silicon mechanical resonators. A focused laser beam was used to pump energy into the motion of the oscillator, to control the frequency response and to provide a carrier signal for the frequency up-conversion. Laser light interaction with the microelectromechanical system (MEMS) was realized through the stress pattern induced within the microfabricated structure by the focused laser beam. Stress-induced stiffening of the oscillator provides control over the effective spring constant and leads to a parametric mechanism for amplification of mechanical vibrations. Periodic modulation of the laser intensity synchronized with the driving force allowed us to demonstrate a degenerate (phase-sensitive) PA scheme with gain in access of 30dB. Design of the oscillator as a part of the built-in Fabry-Perot cavity provides auto-modulation of the effective spring constant as a result of the position-dependent absorption of the light by the oscillator. The auto-modulation mechanism allows a parametric self-excitation induced by continuous wave (CW) laser beam. Self-sustained generation was observed when laser power exceeded a threshold of few hundred microWatts. Nonlinear effects cause frequency dependence vs. laser power, providing a mechanism for frequency modulation of the self-generated vibrations. The same type of optical scheme can also work as an ideal frequency mixer, which combines the self-generated response with an external high-frequency modulation of the laser intensity.

Keywords: MEMS, MOEMS, stress, parametric amplification, modulation, frequency conversion

1. INTRODUCTION

Miniaturization of devices for wireless communication is significantly restricted by the presence of the bulky off-chip components such as quartz resonators, surface acoustic wave (SAW) filters, discrete inductors and varactors. A schematic diagram of the heterodyne transceiver in Fig.1 highlights off-chip elements used in radio frequency (RF) filters, intermediate frequency (IF) filters and voltage control oscillators (VCO). The presence of such elements is dictated by the high quality factor, Q>10,000, required for selection of the desired communication channel, avoiding interference with other numerous users of the communication system. Integrated passive radio frequency (RF) components can provide Q<100 at best, leaving the RF circuit designer face-to-face with millimeter size off-chip components, which interface with IC components at the board level. Modern digital techniques for RF signal processing improve the situation at the expense of complexity and power consumption. A revolutionary approach, based on the implementation of microelectromechanical systems (MEMS) was described by C.T. Nguyen [1]. High frequency, high quality factor (Q~10,000) micromachined silicon oscillators [2,3] are suggested as a replacement for ceramic RF and SAW filters with a few order of magnitude reduction of dimensions of the devices. Arrays of integrated narrow band MEMS RF filters, built into RF low noise amplifiers (LNA) provide a possible base for a novel power-saving transceiver architecture [1,4].

RF MEMS design, proposed by C.T Nguyen [2,3], includes electrostatic drive as a converter of an incoming electric signal into mechanical force applied to a microfabricated silicon oscillator. Resonance response of the oscillator, defined by the modal spectrum of the mechanical structure, is transduced by a capacitive sensor back into electric signal for further processing.

MOEMS and Miniaturized Systems II, M. Edward Motamedi, Rolf Göring, Editors,
Proceedings of SPIE Vol. 4561 (2001) © 2001 SPIE · 0277-786X/01/$15.00

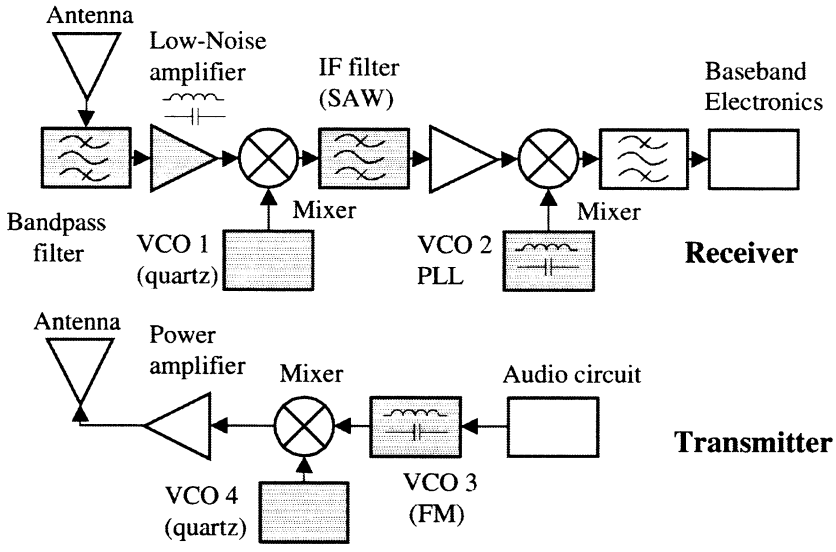

Fig.1: Schematic diagram of a wireless transceiver. Circuits including off-chip components are highlighted.

In the present paper we describe an alternative approach to RF MEMS design. For our device, capabilities of the micromechanical resonator are expanded by interaction with laser light, providing enhanced performance and new functionality. The key concept is engineering the stress induced by the focused laser beam in microfabricated oscillator. The stress energy is transferred then into the energy of the mechanical motion of the oscillator, providing amplification, up to self-generation. The MOEMS oscillator can be modeled by a mass on a spring with a stiffness, which can be controlled by the intensity of the laser beam. That leads the path to optically-induced parametric amplification and puts the basis for numerous implementations of active MOEMS devices making it an analog of an operational amplifier in electronics.

Electrostatic [5,6,7], magnetic [8] and mechanical [9] pumping for parametric amplification in MEMS oscillators have been previously reported. We demonstrate a novel, all-optical approach to parametric amplification, which does not require conducting electrodes or coils located in the proximity of the oscillator.

The same laser beam, which transforms MEMS oscillator into an active device is also used for the detection of the vibration. Interferometric optical detection scheme [10], which significantly relaxes requirements for MEMS design, is implemented by employing the oscillator as one plane of a Fabry-Perot resonator. We demonstrate that this optical scheme provides an auto-modulation of CW laser light, leading to parametric self-excitation. Laser-tuned frequency of the self-generation implies frequency modulation (FM) of the signal. Additional external high frequency modulation (carrier frequency - ω_L) of the incident laser beam allows frequency up-conversion of the self-generated FM MEMS signal (ω_R) into an arbitrary frequency range.

Converting the MEMS oscillator into an active device (while preserving all the functionality of the passive components) can significantly alter RF device architecture. MEMS oscillator would act as an amplifier, filter, VCO, phase detector, frequency modulator and frequency mixer (for up- or down conversion), replacing majority of the RF circuit of the transceiver.

2. OSCILLATORS DESIGN

Two different configurations for high frequency optically driven MOEMS oscillator are presented. The first one, with the resonant frequency ~ 1MHz was designed as a thin disc disk supported by the center pillar. Another, higher frequency structure was developed as a double-clamped beam with submicron cross section. The laser driving-detection technique significantly simplifies the MEMS design, eliminating conductive layers and narrow-gap capacitive pick-up electrodes. The moving part of the oscillator can be done all-single-crystal-silicon, which provides the highest quality factor of the device.

Disc shaped oscillators supported by the center pillar were microfabricated using commercially available silicon-on-insulator (SOI) wafers with a 250 nm thick silicon layer on top of a 1 micron silicon oxide (Fig. 2). Discs of radius R from 5 to 20 microns were defined by electron-beam lithography followed by a dry etch through the top silicon layer. Dipping the resulting structure into hydrofluoric acid undercuts the silicon oxide starting from the disc's periphery toward the center. By timing this wet etch, the diameter of the remaining column of the silicon oxide, which supports the released silicon disc, can be varied.

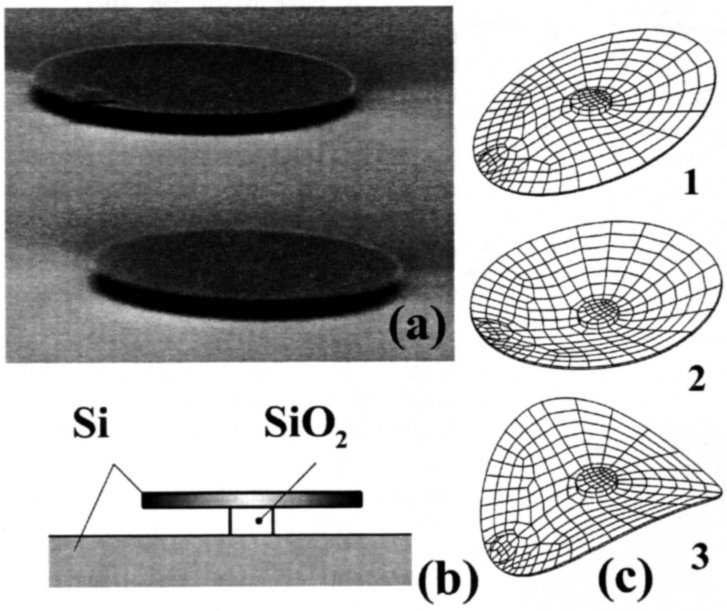

Fig. 2: Scanning electron micrograph of the silicon disc oscillators (a), cross-section of the device (b). First three modes of oscillations are shown, arranged by frequency $f_3>f_2>f_1$ (c).

After a critical point drying (CPD) process, samples were attached to a piezoceramic transducer and placed into a high vacuum chamber ($P=10^{-7}$ Torr). An AC voltage applied to a piezoceramic transducer was used to excite the MEMS oscillators. These oscillations resulted in the variation of the gap between the disc and the silicon substrate and were detected by an interferometric technique with a He-Ne laser beam focused on the surface of the disc. All the measurements were done at room temperature.

Plate vibrations are described by the fourth-order differential equation [11]:

$$\nabla^4\eta + \frac{3\rho(1-s^2)}{Eh^2}\frac{\partial^2\eta}{\partial t^2} = 0 \qquad (1)$$

where E is flexural modulus, s is Poisson's ratio, ρ is the density of the material and h is half-thickness of the plate. Possible solution of the equation (1) are given by the expressions involving Bessel functions J_m, I_m:

$$Y(r,\varphi) = \begin{matrix}\cos\\ \sin\end{matrix}(m\varphi)\left[AJ_m(\gamma r) + BI_m(\gamma r)\right] \qquad (2)$$

Coefficients A, B and γ_{mn} are defined by choosing boundary conditions (displacement and first derivative should be zeroed around the pillar while no bending or shearing forces exist on the circumference of the disc). Figure 2c illustrated three modes of vibrations corresponding to γ_{10}, γ_{00} and γ_{20} marked as 1,2,3 respectively. For our structure (R=20μm, r=6.7μm), the highest quality factor 11,000 was observed for the mode γ_{00} of the disc oscillations with a frequency of 0.89 MHz. Results presented later in this paper are related to this particular resonance.

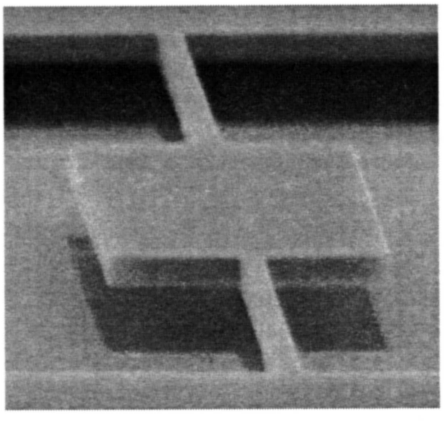

Fig.3 : Paddle oscillator with supporting arms 0.2x0.25x2μm

Another MOEMS oscillator dedicated for the higher frequency range was designed as a double-clamped bridge with submicron supporting arms and a center paddle for increased light absorption (Fig. 3). SOI wafer with 205nm Si top layer on 400 nm SiO_2 was used for microfabrication. Processing and testing are analogous to those, used for disc oscillators. In the present paper we will describe the impact of the laser beam on the translational mode, described by the one-dimensional differential equation

$$EI\frac{d^4y}{dx^4}dx = -\rho A dx\frac{d^2y}{dt^2} \qquad (3)$$

were A is the beam cross-section, and I is cross-sectional moment of inertia.

3. LASER BEAM-INDUCED STIFFNESS MODULATION

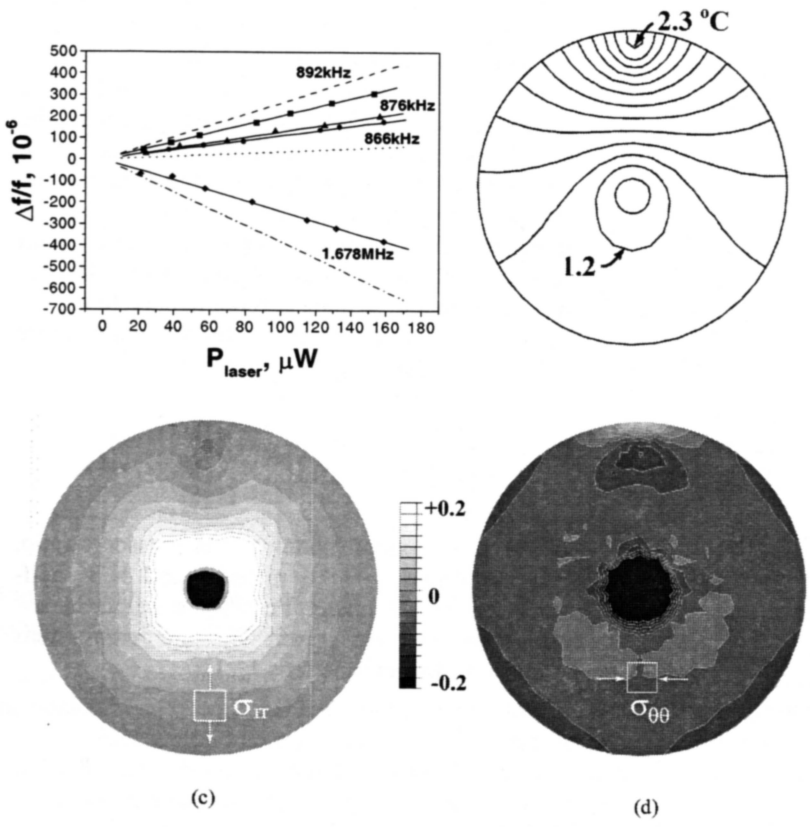

Fig. 4: (a) Relative shift in frequencies versus incident DC laser power. Experimental data (circles correspond to 866kHz resonant peak, triangles - to 876 kHz, squares – to 892 kHz and diamonds – to 1.67MHz) are shown together with linear fits (solid lines). Dotted line, dash and dash-dot lines represent the results of the FEM calculations for the frequency shifts of the modes γ_{01} , γ_{00} and γ_{02} respectively. (b) Temperature field computed from finite element analysis. The model assumes 25% absorption of 260 μW DC laser power over a 5 micron diameter spot at edge of disk. Contour line spacing is 0.1C. (c,d) Two-dimensional stress in radial (c) and hoop (d) directions, induced within the disc by the temperature distribution from Fig. 3b.

A laser beam can affect the behavior of silicon MEMS oscillators by mechanical stress induced either by local heating and thermal expansion [12] or by the photo-generated carriers [13]. In this paper we refer to the former mechanism. Vibrating beam subjected to a tensile force S is described by differential equation:

$$EI\frac{d^2y}{dx^2} = M + Sy \qquad (4)$$

where M is the bending moment produced by transverse loading w. Double differentiating leads to equation:

$$\frac{d^2}{dx^2}(EI\frac{d^2y}{dx^2}) = w + S\frac{d^2y}{dx^2} \qquad (5)$$

Differential equation for transverse vibrations can be obtained by substituting w by inertial force:

$$\frac{d^2}{dx^2}(EI\frac{d^2}{dx^2}) - S\frac{d^2y}{dx^2} = -\rho A\frac{d^2y}{dt^2}$$

Solution for the angular frequency of vibrations for a double-clamped bridge with length L is given by the expression:

$$\omega = \frac{i^2\pi^2 h}{L^2}\sqrt{1+\frac{SL^2}{i^2EI\pi^2}} \qquad (7)$$

which shows square-root tuning of the resonant frequency by the longitudinal force applied. Considering laser heating-induced thermal expansion as a source of the stress, $\sigma = -\alpha E\Delta T$ (α is the coefficient of thermal expansion, and ΔT is the temperature rise), one can write:

$$\omega = \omega_0\sqrt{1-\frac{12\alpha\Delta TL^2}{h^2\pi^2}} \qquad (8)$$

where ω_0 is the frequency when the thermal stress is zero. The frequency shift due to heating of the beam is

$$\frac{1}{\omega}\frac{d\omega}{dT} = -\frac{6\alpha L^2}{\pi^2 h^2} \qquad (9)$$

The relative shift of the resonant frequency should be linear with temperature and this shift is stronger for slender beams (L/h large). As an order of magnitude estimate of $(1/\omega)(d\omega/dT)$, taking L=10 μm, h=0.25 μm, α=2.5*10^{-6}/°C,

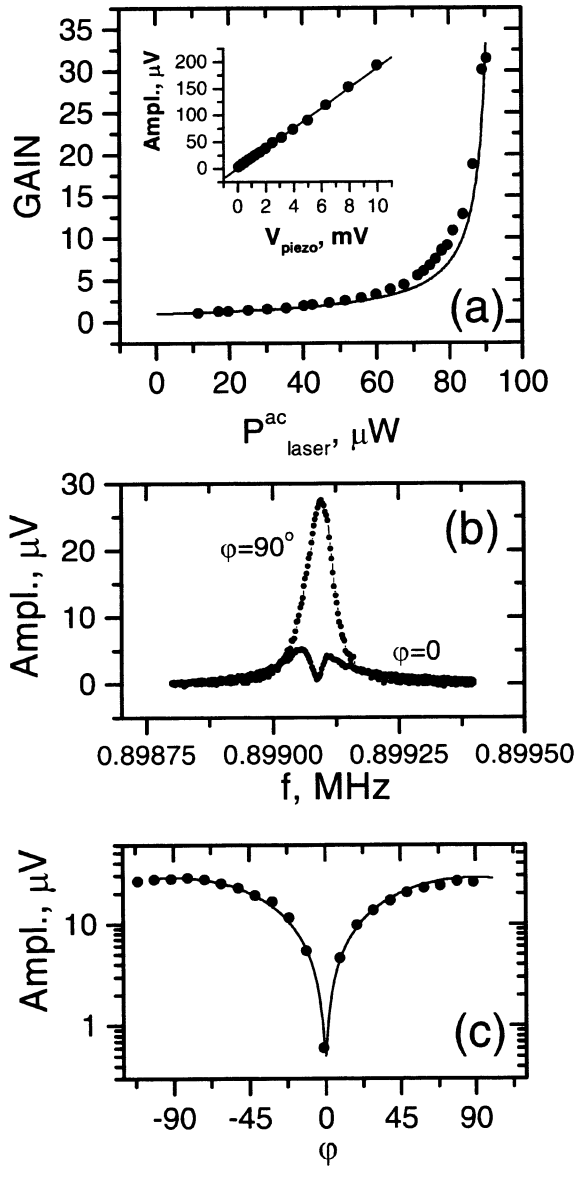

Fig. 5: The parametric amplification gain versus amplitude of the laser power modulation. Experimental points are shown by black circles. The solid line is a fit according to equation (2). The insert shows that the amplified vibrations behave linearly with the piezodriving voltage at a constant optical pump (a). Resonance curves obtained for orthogonal phases of the optical pumping (ϕ=0, ϕ=90°) (b). Amplitude of the resonant peak as a function of the phase shift between piezodrive voltage and optical pump. Experimental results (black circles) are shown together with theoretical fit (solid line) (c)

yields $(1/\omega)(d\omega/dT)$=-0.002/°C. A lumped model of the vibrating beam illuminated by the laser beam would be equivalent to a mass on a spring, whose stiffness is controlled by the laser beam intensity.

Laser beam tuning can also be realized for the disc-shaped oscillator [14]. A low power laser beam (He-Ne, $P_{incident}$~100μW) focused on the periphery of the disc was found to be an effective tool to control the resonant frequency of the disc oscillator. The stiffness variation of the disc is enabled by thermal expansion of the laser-heated periphery of the disc that leads to a significant tensile stress in the radial direction (providing that the central part remains cold due to a heat sink through the short supporting pillar). Under such a stress those vibration modes of the disc, which display primarily radial bending will exhibit a higher resonant frequency in analogy with the increase of the effective spring constant of a prismatic beam under uniaxial tension [11]. Inhomogeneous temperature distribution across the disc makes the situation rather complicated, requiring numerical methods, such as finite element (FEM) analysis. Using the FEM result that ΔT=1.25 °C across the disc for DC power of P_{laser}=260 μW, we arrive at a slope of $5.5*10^{-4}$ /°C for mode 2 in Figure 2c, approximately one-fourth the magnitude of the shift in a beam. Note that in a disk there are two components (radial and hoop) of thermal stress within the disc and that they change in opposition to each other. So in contrast to a beam case, were heating always causes frequency decrease, one can both increase and decrease frequencies by heating the disk. Fig.4a demonstrates experimental data for the frequency shifts for all three modes shown on the vibration spectrum (Fig.2c) as a function of the incident laser power. Modes γ_{00} and γ_{10} demonstrate linear increase of the stiffness with the increased laser power, which is quite counterintuitive. At the same time, an expected decrease of the resonant frequency (i.e. softening) was observed for the high-frequency mode γ_{20}.

The frequencies, temperature and stress in the disk were computed using FEM analysis. Details of FEM calculations can be found elsewhere [14]. Good agreement between the results of FEM calculations and experimental data is demonstrated in Fig. 4a, where the modes γ_{01} and γ_{00} (shapes are shown in Fig.2c) increase in frequency with increasing laser power, while the frequency of the γ_{02} mode decreases with increasing laser power.

4. PARAMETRIC AMPLIFICATION

Control of the effective spring constant, k, of the oscillator by the laser beam opens a path to parametric amplification. Using our microfabricated disc-shaped oscillator we demonstrate the most direct, "textbook" case of a degenerate parametric amplification, usually illustrated by a mass on

spring, whose stiffness undergoes periodic modulation with a frequency twice the frequency of the mechanical motion [15].

The effective spring constant of our disc oscillator was controlled by the intensity of the laser beam, partially modulated by an Electro Optical Modulator (EOM). In order to produce parametric amplification, an increase of the spring constant Δk should occur twice per period, when the deflection of the oscillator is at its maximum, contributing to potential energy $E_p=(k_0+\Delta k)x^2/2$. In our experiment, synchronization of the stiffness modulation with the motion of the oscillator was achieved by using the ac piezodrive voltage V_{piezo} as a reference signal. An external generator provided a double frequency output V_{mod}, phase-locked to the V_{piezo}. After amplification, V_{mod} was used to control the EOM, providing double-frequency modulation of the beam intensity with controlled depth of modulation and phase shift with respect to the reference signal V_{piezo}. The DC component of the laser beam was used for the detection of the oscillations.

Fig. 5a demonstrates the increase of the amplitude of the mechanical vibrations as a function of the amplitude of the ac component in the laser power. The phase shift ($\varphi=90°$) was chosen to provide maximum amplification. The gain was defined as a ratio of the vibration amplitude with laser pumping on and the amplitude of the solely piezo-driven vibrations (when the laser beam has a dc component only). A thirty fold increase of the oscillation amplitude was observed while the modulation of the laser power was increased from zero to $P_{mod}=90$ μW (the amplitude of the local temperature variation under the laser beam was estimated by FEM as 0.25°C). When the pumping power was increased further, self-generation was observed.

The thin line in fig.5a shows the result of calculations based on the expression for the amplitude of the parametrically amplified oscillations [5]:

$$A = F_0 \frac{Q\omega_0}{k_0}\left[\frac{\cos\varphi}{1+Q\Delta k/2k_0} + j\frac{\sin\varphi}{1-Q\Delta k/2k_0}\right] \qquad (10)$$

Here F_0 is the amplitude of the driving force, $F(t)=F_0\cos(\omega_0 t+\varphi)$, Q is quality factor of the oscillator, and the time-varying spring constant is $k(t)=k_0+\Delta k\sin(2\omega_0 t)$. From the results presented in fig.4a we assume a linear dependence of the spring modulation Δk as a function of the laser power modulation P^{ac}_{laser}. The slope $d(\Delta k)/dP^{ac}_{laser}$ was used as a fitting parameter. The insert in fig.5a demonstrates that for the fixed pumping the amplitude of the oscillations is a linear function of the piezodrive voltage, which means that gain is independent of the level of vibrations.

The effect of the phase shift, φ, between the piezodrive and the optical pump is illustrated in fig.5b and 5c. The resonant response for $\varphi=90°$ (maximum amplification) and $\varphi=0$ are shown in fig5b. The suppression of the vibrations at a phase $\varphi=0$ is clearly seen. The amplitude of oscillation as a function of the phase shift φ, shown in fig.5c was fitted by the theoretical expression that must follow from equation (10). Excellent agreement between experimental data (black circles) and the theoretical prediction (solid line) was found.

Phase sensitive low noise parametric amplifier could be the best choice for the phase lock loops (PLL) widely used for frequency demodulation. For a weak telemetry signal the high quality factor of the MOEMS device would allow to reject the noise that is outside the narrow band containing the modulated signal. Feedback loop, adjusting the laser modulation frequency in respect to a source signal will provide demodulated signal.

5. PARAMETRIC SELF-EXCITATION

Modulation of the spring constant of the MEMS oscillator, synchronized with the mechanical motion can be achieved in automatic mode, eliminating the need of the external optical modulator. The fact that our disc or bridge oscillator is a part of the Fabry-Perot cavity (created by the top surface of the silicon wafer and the oscillator) means that all three parameters: reflection, transmission and absorption are position-dependent. Position-dependent reflection is the base for the interferometric detection of the motion. Variation in the absorption within the cycle of oscillations modulates the temperature of the hot spot under the laser beam and can be equivalent to external modulation of the laser beam by EOM.

In order to satisfy the phase relations necessary for the amplification, this built-in Fabry-Perot interferometer should be designed in such a way that any deflection of the oscillator from the equilibrium plane would enhance the tensile stress, rising the stiffness of the oscillator. For the bridge-type oscillator, the proper rest position is at the maximum of the standing wave, created by the incident and reflected laser beams. Any deflection (up or down) shifts the

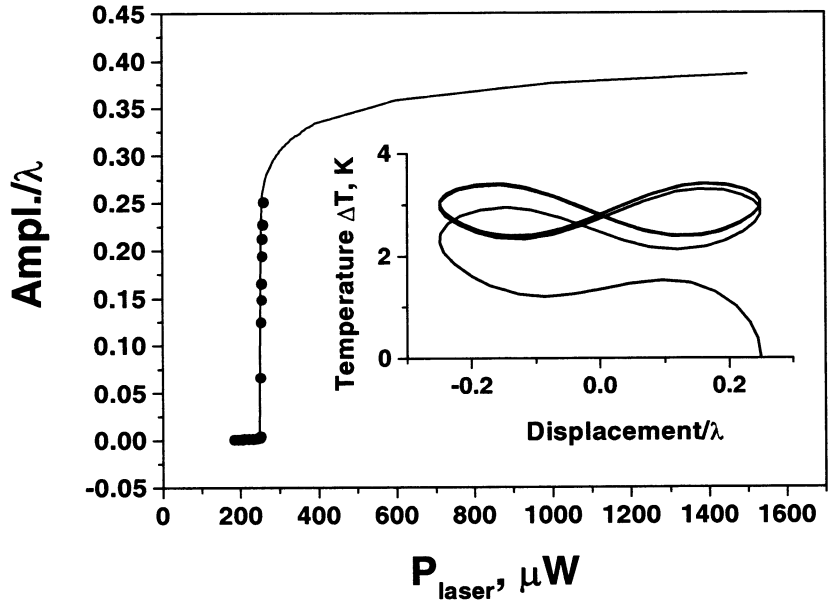

Fig. 6: Amplitude of the self-oscillating peak as a function of the CW laser power. Circles represent experimental data. The result of the theoretical calculations for the amplitude of vibration due to parametric self-excitation is shown by the solid line. Inset demonstrates modulation of the local overheating (disc temperature under the laser beam) caused by the motion within the interferometric pattern. The laser intensity and the ratio of temperature diffusion time to the period of oscillation define the loop area, which is related to the energy income per cycle ($\Delta T \sim \Delta k$, equation (13)).

bridge into a colder zone, rising the resonant frequency. Optical excitation of the γ_{00} vibrating mode of the disc-type oscillator requires opposite arrangement. By placing the disc at the level of the interferometric node (minimum of absorption) one would ensure that any deflection enhances the laser-beam induced radial tensile stress, increasing the effective spring constant of the oscillator.

Insert in Fig. 6 illustrates cyclic temperature variation of the disc caused by the oscillator motion through the interferometric pattern (calculation of $\Delta T(x)$ is described in detail later). Because of the finite decay time of the heat sink through the center pillar, there is a lag in the temperature modulation vs. disc position, which leads to characteristic loops on the temperature-displacement plot. The presence of this loops is a key moment for the parametric self-excitation. The energy income per cycle of oscillations is related to the area of those loops, which is easy to understand by rescaling the temperature variation into a spring constant modulation and taking square of deflection x^2 on the X axis.

In the absence of a driving signal one would expect thermal noise and external vibrations to be amplified by such an auto-parametric mechanism, provided just by a CW laser beam shining on the MEMS device. If the gain in the positive feed-back loop (controlled by the laser power) is high enough to overcome the intrinsic energy losses in oscillator structure – self-generation should occur.

Parametric self-excitation up to self-sustained generation was indeed observed when either disc [16] or bridge oscillator was illuminated by CW laser light (no external modulation). Fig.6 shows the amplitude of self-sustained vibrations of the disc oscillator (no external drive applied) as a function of the power of the HeNe laser beam focused at 5μm spot at the periphery of the disc. An abrupt increase of the vibration amplitude was observed when the light intensity exceeded a well-pronounced threshold at 250 μW.

The oscillations of the disc can be modeled by combining detailed finite element simulations with a simple one-degree of freedom model in which the disc is treated as a mass on a nonlinear spring, and the thermal problem is simplified to a lumped mass with conductive cooling. Expressing time and displacement in dimensionless units, $t = \omega_0 \tau$ and $z = x/\lambda$ respectively, where ω_o is the natural frequency of the relevant mode, and λ is the wavelength of the red laser, the thermal and mechanical problems can be written as

$$\omega_0 \dot{T}(t) = Aq(t) - BT(t), \tag{11}$$

$$\ddot{z}(t) = -\dot{z}(t)/Q - (1 + \Delta k(t)/k_0) z(t) - \beta (1 + \Delta k(t)/k_0)^3 z^3(t), \tag{12}$$

$$\Delta k(t)/k_0 = C(2\omega_0) T(t), \tag{13}$$

$$q(t) = q_0 f(z(t)), \tag{14}$$

where $T(t)$ and $q(t)$ are the time dependence of the heat-induced temperature difference and the absorbed laser power respectively, Q is the quality factor, $\Delta k(t)/k_0$ is the fractional change in effective stiffness and q_0 is the incident laser power. The light intensity distribution function, $f(z)$, represents the position-dependent heat absorption and couples the thermal and mechanical problems. We assume in our model that

$$f(z) = 2\sin^2(2\pi z) \tag{15}.$$

Detailed finite element simulations are used to extract the parameters A,B,C and β. The parameters A and B are estimated from the temperature distribution, assuming that 25% of the laser light intensity is absorbed by the Si disc [16].
The change in stiffness due to laser heating, C, is estimated from results of the FEM simulation by computing the change in resonant frequency at different points in the transient heating cycle, corresponding to different disc displacements. Note that at high frequencies, the temperature modulation away from the point of absorption diminishes considerably, and thus C is a decreasing function of frequency. We find $C(2\omega_0) \approx C(0)/3$ for $\omega_0 = 0.89MHz$.

The cubic nonlinearity parameter, β, is estimated by loading the disc with a uniform pressure, p, and fitting the displacement, z, at the edge of the disc to $p = k(z + \beta z^3)$. We find β=2.3.

The computed temperature variation of the "hot spot" under the laser beam is shown in the inset of Fig.6. In this simulation, the laser power was 250 μW and the system was allowed to evolve freely from an initial deflection. Self-oscillations with the amplitude 0.25λ become a stable state of the system after a few periods. The calculated amplitude of self-generation is plotted against the incident CW laser power as the solid line in Fig.6. The threshold value of 250 μW found by simulation for the onset of the self-sustained oscillation corresponds very well to the experimental data.

Above the threshold power, the amplitude of the self-excited motion of the disc is self-limited by the neighboring interferometric peaks of $f(z)$. As soon as "overexcited" disc overcomes those peaks and invades the negative slope of the absorption (getting colder and softer) – deamplification occurs, preventing further energy accumulation.

Exactly same consideration can be related to the bridge – type MEMS oscillator, providing that inversion of the temperature-stress relation is taken care of by placing the equilibrium plane of the bridge at the maximum of the standing wave, ensuring maximum of absorption at the rest position. A steeper slope of the stiffness-temperature curve makes the structure more responsive to laser light. One can gain a significant increase of the self-generation frequency by scaling down the dimensions of the bridge-type oscillator. The highest frequency of self-generation currently achieved for bridge oscillators is 38 MHz.

Considering operating submicron MOEMS structures, the stability requirements for the optical path overgrow into a real experimental challenge. Design of the integrated on-chip optics is considered as a next step, essential for creation of the real-world-applicable devices.

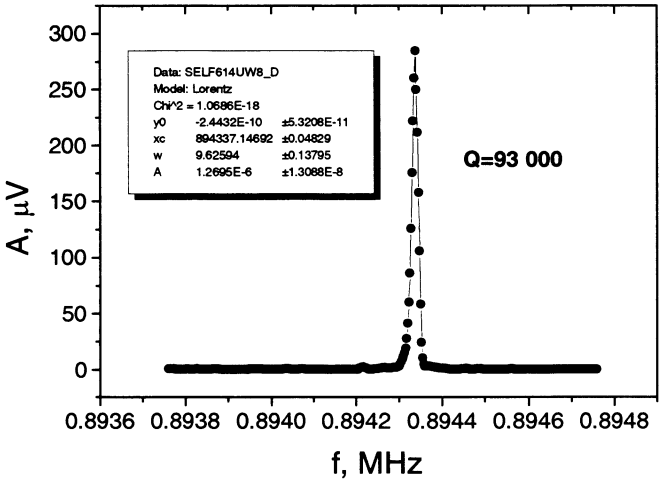

Fig. 7: Spectrum of the signal, self-generated by the disc oscillator (R=20 μm) activated by the HeNe laser beam P_{laser}=244μW

6. FREQUENCY MODULATION AND MIXING

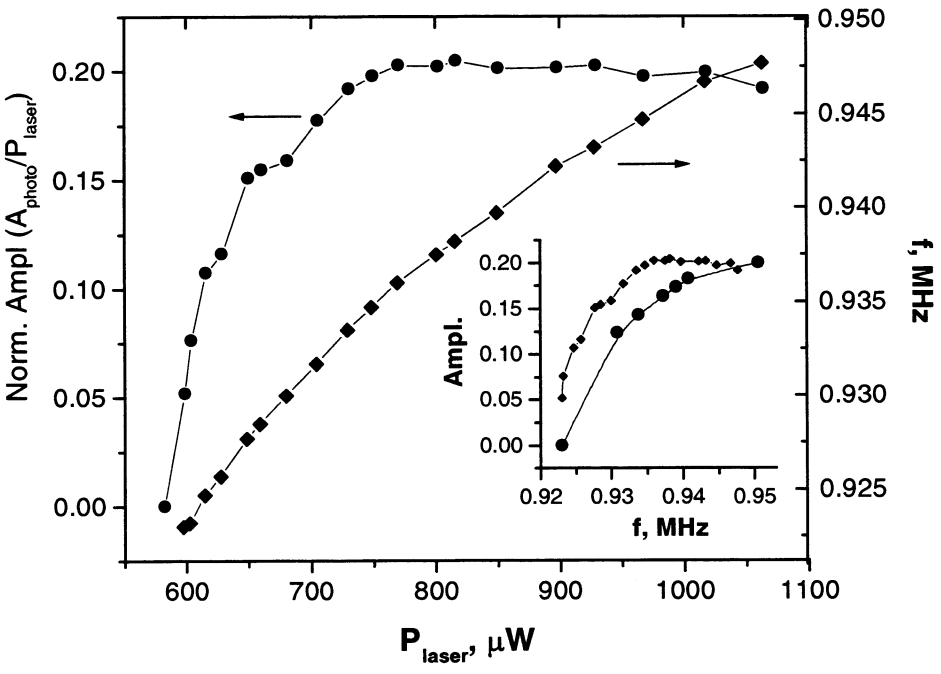

Fig. 8: Frequency and amplitude of self-generated vibrations as a function of the laser power for the disc oscillator (R=19.5 μm). Insert shows plot amplitude vs. frequency: experimental data (diamonds) and results of numerical simulations (circles).

Self-sustained vibrations of MOEMS oscillator can find numerous applications in sensing or RF signal processing. Regarding to wireless communication devices, local oscillator (LO) is the most obvious function, which could be fulfilled by the laser-driven micromechnical resonator. Fig.7 shows the spectrum of self-sustained vibrations for the disc-shaped oscillator (R_{out}=20μm, R_{pillar}=6.7μm). The line width Δω~10 Hz (Q~100,000) seems to be limited by the resolution bandwidth of the spectrum analyzer. It should be mentioned however, that long-time average of the acquired spectrum can lead to significantly broader resonant peak Δω~100 Hz, which is attributed to laser beam drifting within the MEMS structure. Important application – laser tuned generator (analog of the voltage controlled oscillator - VCO) can arise from the sensitivity of the MEMS oscillator to the laser beam power. Fig. 8 shows amplitude and frequency of self-sustained vibrations of the disc R_{out}=19μm, R_{in}=4.7μm for the laser power range over the self-generation threshold. Significant shift of the generated frequency (Δf~3%) has been observed along with the step-like increase of the amplitude (from zero to interference-limited λ/4) when the laser power was increased from the threshold value (580μW) to 1.1mW.

The physical reason for the frequency increase is the non-linear term in equation (12). Non-linearity is caused both by finite thickness of the oscillator and by the position-dependent light absorption, which show up as a deflection-dependent stiffness. The MEMS oscillator can be described as a mass on a nonlinear "hard" spring. A dramatic increase of the amplitude of oscillations in the self-generating regime makes the oscillator effectively stiffer. By plotting amplitude of oscillations vs. frequency, typical behavior for non-linear oscillator [18] can be observed. Insert in Fig.8 shows amplitude-frequency dependence observed experimentally (diamonds) along with the numerical solution of the equation system (11-15). Qualitatively, the frequency behavior of the disc oscillator is in a good agreement with the result of numerical simulations, however, the value of β=0.375 used for the best fit, differs from the result of FEM calculations. Detailed analysis of the non-linear parametrically self-excited oscillations is currently in progress.

Frequency modulation of the signal, self-generated by MEMS oscillator can be easily implemented by modulating the laser power (similar effect is expected from tuning the laser wavelength). From Fig. 8 one cam see that our prototype device will provide modulation depth of 25 kHz over 0.95MHz base frequency. Such a modulation depth is comparable with what is commonly used for FM broadcasting, although 1 MHz carrier frequency seems to be too low.

The standard way to rise the carrier frequency is a mixing or up-conversion. FM signal is commonly prepared at some convenient frequency and then shifted to any desired range. Switching mixer or general non-linear element can be used to form a product of the source signal (ω_R from FM) and signal from the high-frequency local oscillator at ω_L, creating combination frequencies at the resulting spectrum:

$$\sin(\omega_R t)\sin(\omega_L t) = 1/2[(\cos(\omega_R - \omega_L)t - \cos(\omega_R + \omega_L)t]$$

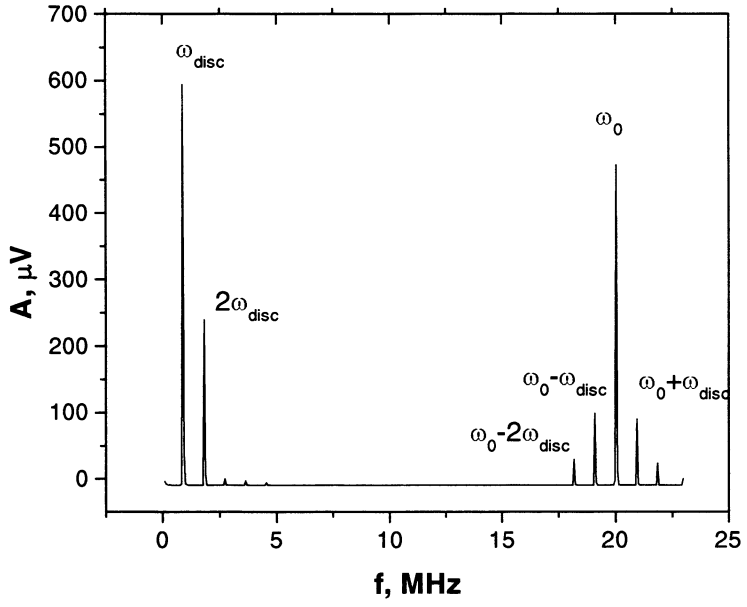

Fig. 9: Wide range spectrum resulting for the mixing of the self-generated signal (f=0.89 MHz) and external modulation of the laser beam (f_{mod}=20MHz)

Generally, only one of those combination frequencies is later selected by a band-pass filter for broadcasting.

MOEMS oscillator is a ready-to-use ideal mixer, since the intensity of the reflected light is a product of the incident light intensity and reflectivity of the MEMS oscillator. By modulating the power of the laser beam at high frequency, ω_L (far above the modal spectrum of the mechanical device), one provides that the signal spectrum at the photo receiver will contain up-shifted ($\omega_R+\omega_L$) and down-shifted ($\omega_R-\omega_L$) components.

A wide-range spectrum of the signal at the photoreceiver, shown in Fig.9 was acquired when 40 μm disc (eigenfrequency 0.9MHz) was set in self-generation by a laser beam, partially modulated at 20MHz frequency. Self-generated peak together with the second harmonic are linearly transferred into the high-frequency domain

Up-conversion can be combined with the frequency modulation (described above), if in addition to high-frequency modulation at ω_L the laser power (or laser wavelength) is modulated by low-frequency signal (for example, audio signal). In that case MOEMS would substitute FM, LO and mixer – practically the whole RF circuit of the transmitter, except antenna power amplifier.

7. DESIGN COSIDERATIONS

Increasing the resonant frequency of the MOEMS device and reducing the laser power required for an optical excitation would be the general way to expand the applicability of MOEMS devices. Since the modulation of the laser heating-induced stress is the basis of functionality of our devices, the upper frequency limit can be estimated from the heat propagation time. Assuming that dimensions of the silicon structure are reduced down to a laser beam spot size R~1μm, one can estimate the heat relaxation time as τ_{heat}~R^2/D_{Si}=10 nsec (D_{Si} is a thermal diffusivity in silicon). As it was described in section 5, the energy income per oscillator cycle is defined by the area of the loops in a graph Δk vs. deflection x. Those loops originate from the fact that the temperature change is in a lag in respect to the mechanical motion. Making the thermal system too inertial would diminish thermal modulation, transforming Δk(x) loops into a horizontal line with zero area. Laser pumping is a pure MEMS effect, based on the fact that heat transfer can be extraordinary fast in microscopic objects. Optimization of the MEMS oscillator design aiming at the enhanced sensitivity $\Delta k/P_{laser}$ can extend the working range of the resonant frequency up to f~1/ $10\tau_{heat}$, covering the frequency region up to 1GHz. Numerical simulations aiming at the optimum high frequency – low threshold design for the optically pumped oscillator are currently in progress.

8. CONCLUSION

High frequency (f~1MHz), high quality factor (Q=11,000) single crystal silicon micromechanical oscillators were fabricated in a novel design with cylindrical symmetry. It was shown that a low power (P~100μW) laser beam focused at the periphery of the disc can tune the resonant frequency of the oscillator. Using double-frequency modulation of the laser beam power, we have achieved parametric amplification of the mechanical vibrations. A gain of up to 30 and the expected phase dependence of a parametric amplifier were demonstrated.

Parametric self-excitation was demonstrated by auto-modulation of the CW HeNe laser beam. This auto-modulation was realized by implementing the moving part of the MEMS oscillator as a part of Fabry-Perot interferometer. Self-sustained vibration of the disc was observed when the CW laser power exceeded a threshold value of 250 μW. Self-generation, excited by CW laser light was also obtained for the higher frequency (currently up to 38 MHz) bridge-type oscillators.

We demonstrate that microfabricated light-activated high frequency MOEMS can function as amplifiers, phase detectors (demodulator), light-controlled oscillator (frequency modulator) and frequency converter in RF circuits, replacing off-chip components in wireless communication devices.

ACKNOWLEGMENTS

The authors are grateful to Ai-Chi Chien for assistance with the FEM computations and to the staff at Cornell Nanofabrication Facility for generous aid in fabrication. This work was supported by the Cornell Center for Materials Research (CCMR), a Materials Research Science and Engineering Center of the National Science Foundation (DMR-0079992). Particular acknowledgment is made of the use of the Research Computing Facility of the CCMR.

REFERENCES

1. C. T.-C. Nguyen, "Micromechanical components for miniaturized low-power communications (invited)," *Proceedings*, 1999 IEEE MTT-S International Microwave Symposium RF MEMS Workshop (on Microelectromechanical Devices for RF Systems: Their Construction, Reliability, and Application), Anaheim, California, June 18, 1999, pp. 48-77
2. C. T.-C. Nguyen, A.-C. Wong, and H. Ding, "Tunable, switchable, high-Q VHF microelectromechanical bandpass filters," *Digest of Technical Papers*, 1999 IEEE International Solid-State Circuits Conference, San Francisco, California, Feb. 15-17, 1999, pp. 78-79, 448.
3. Wan-Thai Hsu, John R. Clark and Clark T.-C. Nguyen "A submicron capacitive gap process for multiple-metal-electrode lateral micromechanical resonators" Technical Digest MEMS 2001 The 144 IEEE International Conference on MEMS, Interlaken, Switzerland Jan, 21-25, 2001, pp. 349-352
4. C. T.-C. Nguyen, "Micromechanical filters for miniaturized low-power communications (invited)," to be published in *Proceedings of SPIE*: Smart Structures and Materials (Smart Electronics and MEMS), Newport Beach, California, March 1-5, 1999, 12 pages.
5. D. Rugar and P. Grutter Phys. "Mechanical parametric amplification and thermomechanical noise squeezing" Rev. Lett **67**, 699 (1991)
6. D.W. Carr, S. Evoy, L. Sekaric, H.G. Craighead and J.M. Parpia, "Parametric amplification in a torsional microresonator" Appl. Phys. Lett. **77**, 1545, (2000)
7. A. Olkhovets, D.W. Carr, J.M. Parpia and H.G. Craighead "Non-Degenerate Nanomechanical Parametric Amplifier" IEEE Intl. Conference on Micro Electro Mechanical Systems MEMS 2001, Interlaken, Switzerland, January 21-25, 2001
8. W.M. Dougherty, K.J. Bruland, J.L. Garbini and J.A. Sidles "Detection of AC magnetic signals by parametric mode coupling in a mechanical oscillator", Meas. Sci. Technol. **7**, 1733 (1996)
9. A. Dana, F. Ho, Y. Yamamoto, "Mechanical parametric amplification in piezoresistive gallium arsenide microcantilevers" Appl. Phys. Lett. **72,** 1152 (1998)
10. D.W. Carr, L. Sekaric and H.G. Craighead, "Measurement of nanomechanical resonant structures in single-crystal silicon" J. Vac. Sci. Technol. B **16**, 3281 (1998).

11. P.M. Morse "Vibration and sound" 2-nd edition, McGraw-Hill Book Company, Inc., New York, pp. 172-216, (1948)
12. S. Timoshenko, D.H. Young and W. Weaver, "Vibration Problems in Engineering", 4th edition, John Wiley and Sons, New York, pp. 453-455, (1974)
13. P.G. Datskos, S, Rajic, I. Datskou "Photoinduced and thermal stress in silicon microcantilevers" Appl. Phys. Lett. **73,** 2319 (1998)
14. M. Zalalutdinov, A. Olkhovets, A. Zehnder, B. Ilic, D. Czaplewski, H.G. Craighead and J.M. Parpia, "Optically pumped parametric amplification for micromechanical oscillators" Appl. Phys. Lett. **78**, 3142-3144 (2001)
15. W.H Louisell "Coupled mode and parametric electronics" John Wiley & Sons, Inc. New York (1960)
16. M. Zalalutdinov, A. Zehnder, A. Olkhovets, S. Turner, L. Sekaric, B. Ilic, D. Czaplewski, H.G. Craighead and J.M. Parpia, "Auto-parametric optical drive for micromechanical oscillators" Appl. Phys. Lett. 79, 695-697 (2001)
17. Gray, D.E., editor, American Institute of Physics Handbook, 3rd edition, McGraw-Hill, pp. **6**-118-**6**-156, (1972). Absorption calculation assumes optical properties of pure Si at 620nm.
18. Ali H. Nayfen, D.T. Mook "Nonlinear Oscillations" Pure and Applied Mathematics, A-Wiley pp. 161